Volume 14
Number 48
28 December 2022
Pages 5021–5112

Analytical Methods

rsc.li/methods

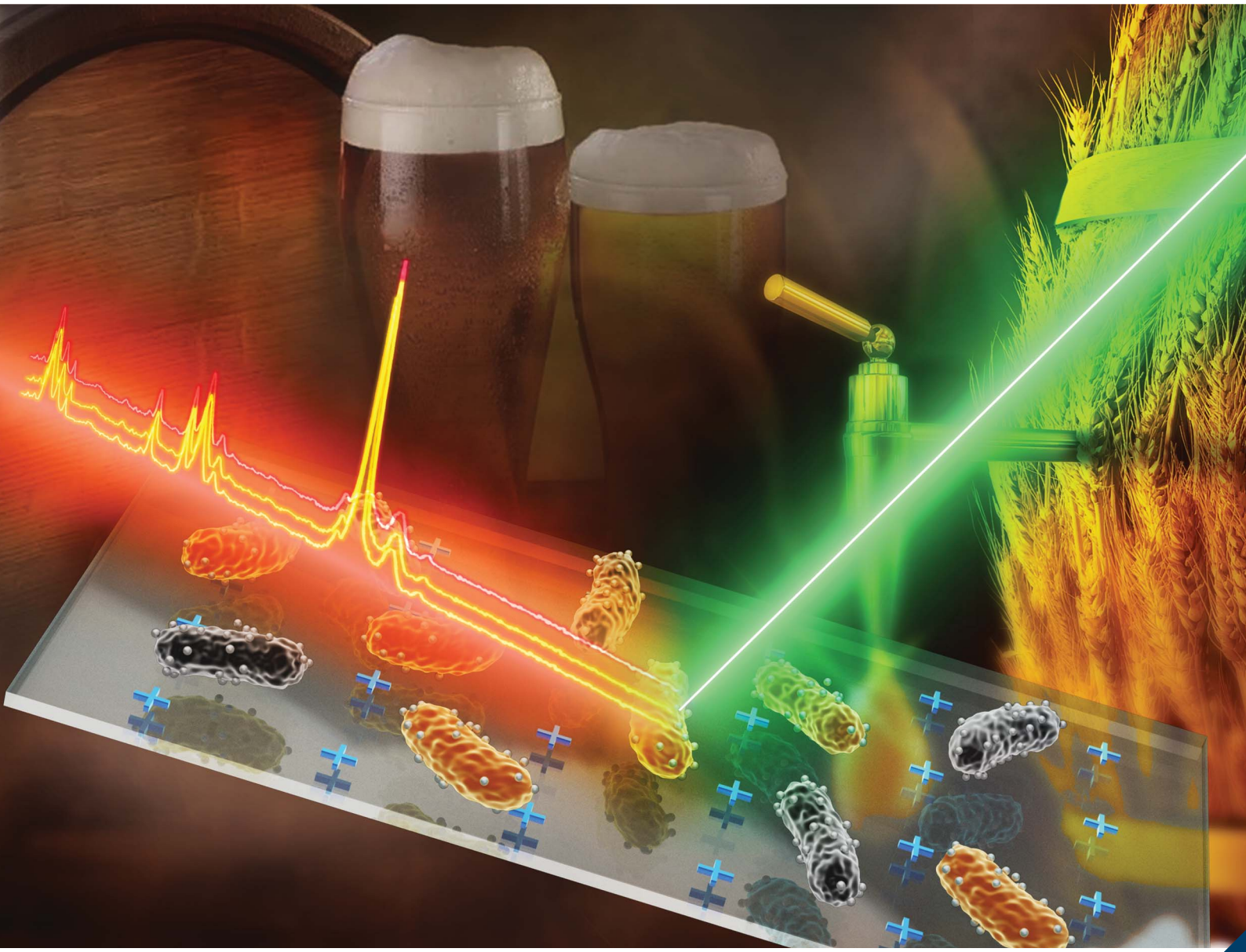

ISSN 1759-9679

ROYAL SOCIETY OF CHEMISTRY

PAPER
Bei Li *et al.*
Rapid detection of beer spoilage bacteria based on label-free SERS technology

Analytical Methods

ROYAL SOCIETY OF CHEMISTRY

PAPER

View Article Online
View Journal | View Issue

Cite this: *Anal. Methods*, 2022, **14**, 5056

Rapid detection of beer spoilage bacteria based on label-free SERS technology

Lindong Shang,[ab] Lei Xu,[d] Yu Wang,[ab] Kunxiang Liu,[ab] Peng Liang,[ab] Shuangjun Zhou,[e] Fuyuan Chen,[ab] Hao Peng,[ab] Chunyang Zhou,[f] Zhenming Lu[d] and Bei Li*[abc]

Received 31st July 2022
Accepted 4th November 2022

DOI: 10.1039/d2ay01221a

rsc.li/methods

Beer spoilage bacteria have been a headache for major breweries. In order to rapidly identify spoilage bacteria and improve the sensitivity and signal-to-noise ratio of bacterial SERS detection, the label-free SERS technique was used as a starting point, and we found eight bacteria species that led to beer spoilage. The impact of AgNP concentration and AgNP and bacterial binding time on the final results were thoroughly investigated. To maximize the increase in the SERS signal, an aluminized chip was created. We merged the t-SNE reduced dimensional analysis algorithm, and SVM, KNN, and LDA machine learning algorithms to further investigate the effect of the approach on the final identification rate. The results demonstrate that SERS spectra had an increased intensity and signal-to-noise ratio. The machine learning classification accuracy rates were all above 90%, indicating that the bacteria were correctly classified and identified.

Introduction

Beer has long been thought to be a safe drink. Beer is not an optimal development habitat for many microbes due to the presence of alcohol, bitter hop compounds, high carbon dioxide concentrations, low pH, low dissolved oxygen, and very limited levels of nutrients.[1,2] Some microbes, though, can still grow in it. The presence of these beer spoilage bacteria can result in a reduction in beer quality as well as financial losses for the brewery. Most of the beer spoilage bacteria are lactic acid bacteria,[3] such as *Levilactobacillus brevis*, and they are exclusively heterogeneous fermenters, resistant to hops, ideal for a wide range of growth, capable of fermenting dextrin and starch, and prone to overfermentation of the fermentation broth.[4] *Lactiplantibacillus plantarum* decreases the pH of beer, causing the concentration of diethylstilbestrol to exceed the normal limit, resulting in precipitation or hazy material and a foul flavor. As a result, identifying bacteria has become a pressing issue that must be addressed promptly in the fermentation process. Traditional methods of bacterial identification, such as colorimetric methods,[5,6] plate culture methods,[7] flow cytometry,[8] polymerase chain reaction (PCR),[9] and enzyme-linked immunosorbent assay (ELISA),[10] have accurate results but take 2–3 days to complete, which does not meet the requirement for real-time detection of beer spoilage bacteria in the beer brewing process. Bioassays with a shorter analysis time and improved sensitivity must be developed.

The Raman spectroscopy technique is widely used for the detection of various bacteria because of its advantages such as fast detection speed and specificity of spectral peaks.[11] However, as compared to fluorescence and electrochemical approaches, the Raman technique has limitations, such as a low spectrum intensity. Furthermore, because of the complicated microbial growth environment in the beer brewing process, the resulting spectra frequently contain a high amount of fluorescent background interference during Raman detection,[12] which has a significant impact on the spectral resolution. As a result, the key issue is to improve the sensitivity and spectrum intensity of Raman spectra. Surface enhanced Raman spectroscopy (SERS) has faster detection speed and spectral specificity, which can provide stable and clear bacterial fingerprints in complex sample environments with less fluorescence background interference.[13] There are generally two types of bacterial SERS detection methods: label-based methods and label-free methods;[14,15] although label-based methods have high sensitivity and speed, the capture and labeling steps are dependent on antibody or aptamer recognition. Moreover, antibodies produced by immunized animals are expensive and poorly reproducible.[16] It is difficult to find aptamers with high

[a]*State Key Laboratory of Applied Optics, Changchun Institute of Optics, Fine Mechanics and Physics, Chinese Academy of Sciences, Changchun, 130033, P. R. China. E-mail: beili@ciomp.ac.cn; Tel: +86-0431-86708966*

[b]*University of Chinese Academy of Sciences, Beijing 100049, P. R. China*

[c]*HOOKE Instruments Ltd, Changchun, 130031, P. R. China*

[d]*National Engineering Research Center for Cereal Fermentation and Food Biomanufacturing, Jiangnan University, Wuxi, 214122, P. R. China*

[e]*Department of Chemistry, Yanbian University, Park Road 977, Yanji 133002, Jilin Province, P. R. China*

[f]*College of Life Sciences and Technology, Changchun University of Science and Technology, Changchun, 130022, P. R. China*

cooperativity, and the binding period to the target bacteria is long.[17] Here, our study will focus on label-free methods.

Label-free methods are highly sensitive and require low-cost metal nanoparticles (colloidal suspensions) making them ideal for mass promotion.[18] Furthermore, *in situ* produced silver nanoparticles (AgNPs) can maintain close contact with bacterial membranes,[19,20] allowing for label-free detection at the single-cell level regardless of bacterial taxonomic variety, growth stage, physiological state, or culture conditions. Label-free SERS detection of bacteria has received increasing attention in recent years. Piyanan Chuesiang[21] used commercial silver nanoparticles and investigated the effect of silver nanoparticles on the SERS spectral identification results of *E. coli* and *Salmonella* with different particle sizes and different coating agents. Muhammad Kashif[22] explored a variety of bacteria in the food industry using a nanosilver synthesis method with sodium citrate. The results were validated using the PCA + PLS-DA algorithm, which finally allowed the classification of bacteria. However, fewer reports have been published for beer spoilage bacteria. The production of nanoparticles and the conditions of binding nanoparticles and bacteria are most likely to be neglected by researchers, resulting in a low signal-to-noise ratio of the SERS spectra of bacteria obtained by most of them and indirectly leading to a low final identification rate.

Inspired by the above results, to identify beer spoilage bacteria and increase the sensitivity and signal-to-noise ratio of bacterial SERS detection, a label-free SERS approach was used. We collected eight species of bacteria associated with beer spoilage, looked at the impact of the AgNP concentration and AgNP binding time with bacteria on the final results, and made aluminized chips to boost the SERS signal even more. To further investigate the effect of the method suggested in this study on the final identification rate, we integrated it with the t-SNE method for downscaling analysis and used SVM, KNN, and LDA machine learning algorithms for analysis and prediction. The results of the experiments reveal that the method not only produces SERS spectra with a higher intensity and signal-to-noise ratio but also successfully classifies and identifies beer spoilage bacteria.

Materials and methods

Materials and instruments

Hydroxylamine hydrochloride ($NH_2OH \cdot HCl$), sodium hydroxide (NaOH), silver nitrate ($AgNO_3$), potassium chloride (KCl), and rhodamine 6G (R6G), were purchased from Sigma-Aldrich Corporation. Glass slides (26 mm × 76 mm × 1 mm), centrifuge tubes (10 mL), disposable filters (0.22 μm), and syringes were purchased from Millipore Company. A Milli-Q pure water system, METTLER TOLEDO-T electronic analytical balance, SH SCIENTIFIC IS-A29 constant temperature shaking incubator, Thermo Scientific Megafuge 8R refrigerated centrifuge, SCILOGEX SCI-VS vortexer, Zetasizer nanoparticle particle size potentiometer, Malvern PANalytical and SHIMADU-UV2550 UV-vis absorption spectrometer were used. Raman spectra were collected using a Raman spectrometer (Hooke Instruments Ltd., P300). The beer spoilage bacteria utilized in the experiment, such as *Levilactobacillus brevis*, *Lentilactobacillus buchneri*, *Lactiplantibacillus plantarum*, *Lactobacillus reuteri*, *Lactiplantibacillus pentosus*, *Lactobacillus helveticus*, *Lactobacillus acidophilus*, and *Limosilactobacillus fermentum*, were isolated and identified from genuine samples by Jiangnan University's National Engineering Research Center for Cereal Fermentation and Food Biomanufacturing.[23]

AgNP fabrication and characterization

The enhanced Leopold and LendI technique[24] was used to manufacture AgNPs. To generate a 10 mL (0.01 mM) silver nitrate solution, 1 mL silver nitrate solution (0.1 mM) was diluted with 9 mL deionized water. After that, 100 mL of deionized water was mixed thoroughly with 11.6 mg of hydroxylamine hydrochloride (0.17 mM) and 3.3 mL of sodium hydroxide solution (0.1 M). Finally, the prepared silver nitrate solution was mixed three times with the reducing agent, shaking each injection for 5 s. The gray-green AgNPs were generated almost instantaneously, and then reacted on a shaker at 200 rpm for 30 min to allow complete reaction of the substrate. After the reaction is finished, it was placed in a 4 °C refrigerator for 30 min to crystallize the unreacted dissolved materials and assure the purity of the AgNPs. Then it was filtered through a 0.22 μm Millipore filter membrane, sealed, and kept refrigerated at 4 °C to keep it away from light. This method was used to obtain AgNPs@normal (the concentration of AgNPs was obtained as 0.88 μM). This process produces AgNP sol that can be kept for about a month. AgNPs in a modest quantity for optical characterization, a sample was obtained and placed in the transmission electron microscope (TEM), ultraviolet-visible absorption spectrometer, and Zetasizer nanoparticle size potentiometer. The aggregation of AgNP sol can be aided by KCl, NaCl, and other salt solutions.[25] When combining silver nitrate solution and a reducing agent to make AgNP sol, we add 0.3 mL of KCl solution (0.03 mM) to make the resulting solution AgNPs@KCl.

Fabrication of aluminized glass slides

Before the Raman test, the glass slides were treated with anhydrous ethanol and deionized water ultrasonication for 5 min to remove organic matter and impurities from the glass surface and then blown dry with nitrogen. Subsequently, an aluminum film was laid flat on the surface of the slides by vacuum vapor deposition and they were then stored in a refrigerator at 4 °C after cooling.

Pretreatment of bacteria

To demonstrate the bacterial pretreatment procedure, this article uses *Lactiplantibacillus plantarum* as an example. The *Lactobacillus* strains were placed in a 250 mL culture flask with 100 mL inactivated de Man Rogosa Sharpe (MRS) medium (pH 6.2) and incubated for 64 h at 37 °C at 200 rpm in a rotary shaker. The *Lactobacillus* strains were washed with deionized water after cultivating them to remove the culture media. 50 μL of bacterial solution was taken in 1 mL deionized water, mixed with a vortexer, centrifuged in a centrifuge (4 °C, 8000 rpm, 5

min), and the supernatant was removed, and the process was repeated three times with 1 mL deionized water. After cleaning, 1 mL of deionized water was added, vortexed, and stored at 4 °C for subsequent use.

Preparation of AgNPs & bacteria

To explain the synthesis process of AgNPs and bacteria, this article uses farmed *Lactobacillus* strains as an example. First, a vortexer is used to equally shake the cleansed bacteria and AgNPs@KCl. Then 30 μL was placed in a tube, followed by the equivalent quantity of 30 μL of AgNPs. AgNPs@KCl was promptly added to the centrifuge tube, stirred uniformly with a vortexer, and then placed in a constant temperature shaker for incubation at 37 °C and 200 rpm. Imaging and Raman measurements were carried out on metal slides using a 100× objective lens.

SERS enhanced verification

After the fabrication of AgNPs, the enhancement effect was first verified. 100 μL diluted rhodamine 6G (1×10^{-8} M) was mixed with 100 μL of AgNPs@normal (AgNPs@KCl) colloidal solution for 5 min, and then 5 μL of the above samples was dropped onto the treated aluminum-plated slides for SERS signal detection with a laser power of 0.1 mW and integration time of 0.1 s (Fig. 1(b)).

The effect of the AgNP concentration on the enhancement effect

10 mL of the produced AgNPs@KCl was taken by injecting deionized water to obtain a AgNP colloid after different concentration gradient dilutions. Then 10 mL of AgNPs@KCl was taken with the centrifuge, and centrifuged for 5 min at 10 000 rpm; after centrifugation, half of the supernatant was extracted and mixed well using a vortexer to obtain different concentrations of AgNP solution after gradient concentration. Different concentrations of AgNPs and bacteria were mixed and placed under a 100× objective lens with a laser power of 3 mW and integration time of 2 s to test the SERS spectrum signal.

Effect of reaction time on the results

A 5 mL sample of AgNPs@KCl & bacteria was shaken at 200 rpm at 37 °C in a shaker. The SERS spectrum signal was evaluated at each time slot by placing 5 μL of the sample on an aluminum-plated slide according to the response time and placing them under a 100× objective lens with a laser power of 3 mW and integration time of 2 s.

Identification of various *Lactobacillus* strains

20 μL of each of the various beer spoilage bacteria (*Levilactobacillus brevis*, *Lactiplantibacillus plantarum*, *etc.*) and AgNPs@KCl was taken after treatment, mixed with a 1 : 1 ratio, and incubated at 37 °C for 4 h on a constant temperature shaker; 5 μL of each of these samples was dropped on an aluminum-plated slide, and SERS detection was performed under a 100× objective lens, with a test laser power of 1 mW and integration time of 2 s, and 100 spectra were collected for each species of bacteria. The results were obtained and then validated using the t-distributed stochastic neighbor embedding (t-SNE) downscaling analysis algorithm,[26] and support vector

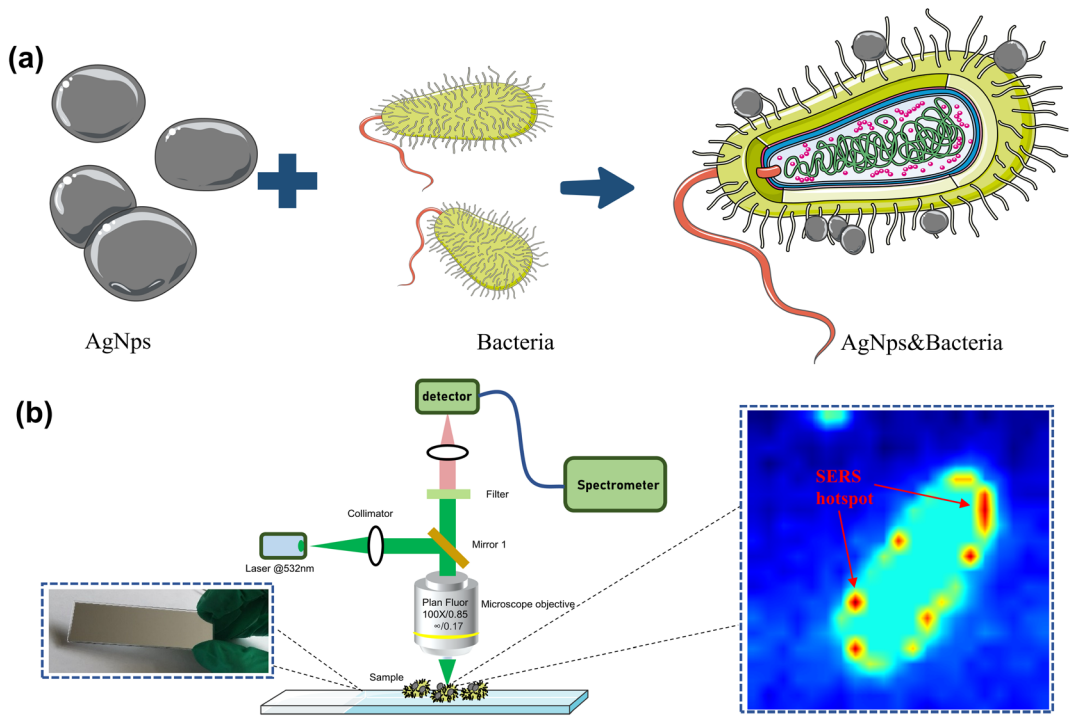

Fig. 1 (a) The overall flow chart of the experimental test. (b) The optical path diagram of the SERS test, in which aluminized glass slides are used, and the SERS hot spot diagram is also shown in the figure.

machines (SVM),[27] K-nearest neighbor (KNN),[28] and linear discriminant analysis (LDA)[29] machine learning algorithms for predictive analysis of the results.

Validation analysis of fermentation-contaminated beer

Samples of uncontaminated beer were extracted from the fermentation process. Two beer spoilage bacteria, *Levilactobacillus brevis*, and *Lactiplantibacillus plantarum* were added to simulate the actual contaminated beer bacterial environment. After incubation in a 37 °C incubator for 1 day, single-cell Raman spectra were collected following the normal SERS assay procedure for beer spoilage bacteria. The acquired spectra were then input to build the best spoilage strain classification model, and we could output the class and predicted score of single cells.

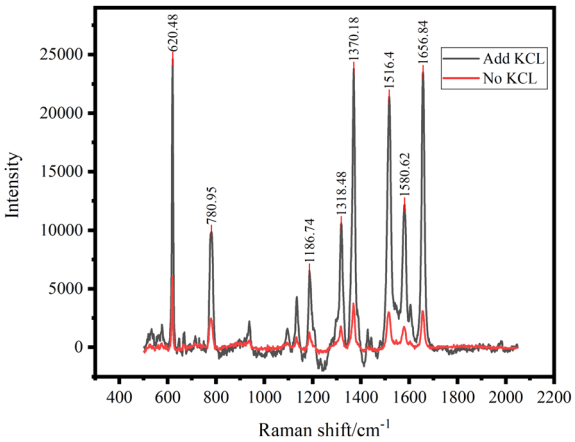

Fig. 3 Comparison diagram of the rhodamine signal strength (the black line is the comparison curve with KCl added and the red line is the comparison curve without KCl added).

Results and discussion

Characterization of AgNPs

The results of AgNPs' optical characterization are displayed in the following Fig. 2: the TEM plots (Fig. 2(a)), can be used to more clearly determine the nanoparticles' diameter, which is in the range of 40–70 nm. This conclusion can also be verified from the DLS (dynamic light scattering) plots (Fig. 2(d)), where the diameter of the nanoparticles are seen to be around 60 nm in the DLS curves. From Fig. 2(b), it can be seen that the AgNPs and bacterial binding bimodal peaks are obvious and the AgNP particles are of good quality. The ZETA potential in Fig. 2(c) is 18.07ζ, which is due to the addition of KCl during the fabrication of AgNPs increasing its aggregation.

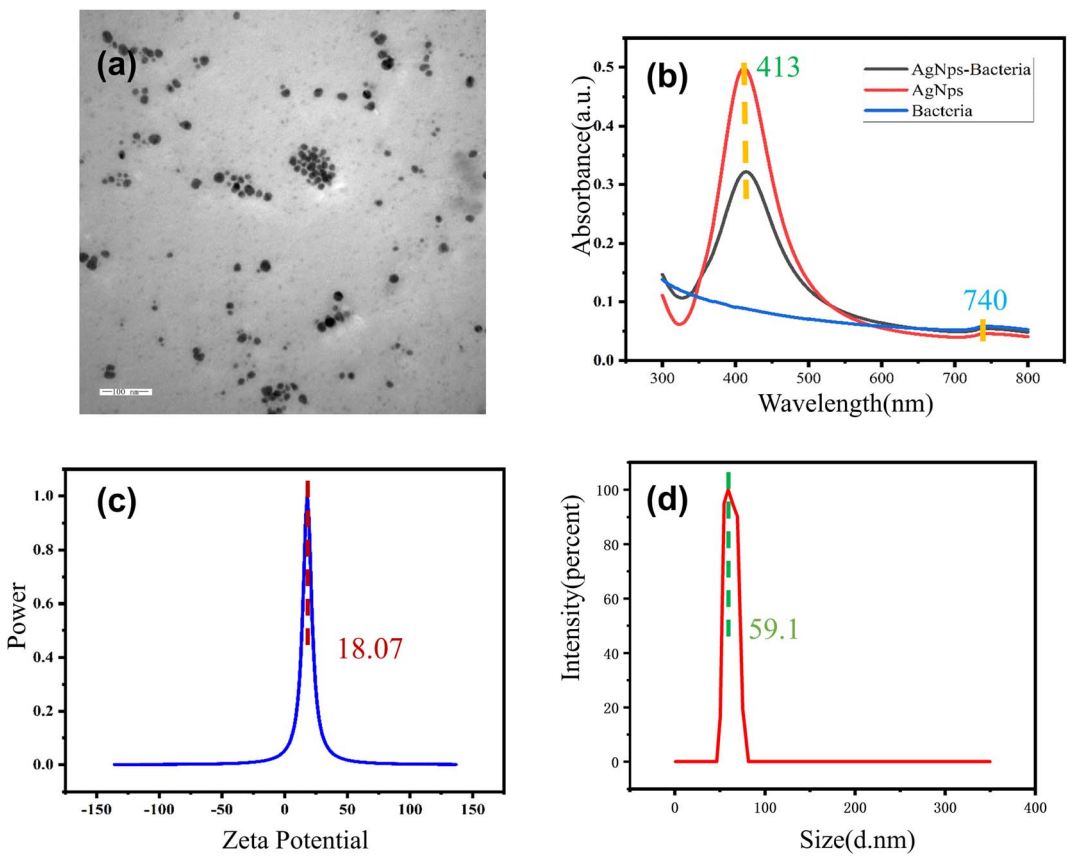

Fig. 2 Optical characterization of silver nanoparticles. (a) The TEM diagram of AgNP particles, (b) the UV-vis absorption spectrum of AgNP particles, (c) the zeta potential diagram of AgNP particles, and (d) the DLS diagram of AgNP particles.

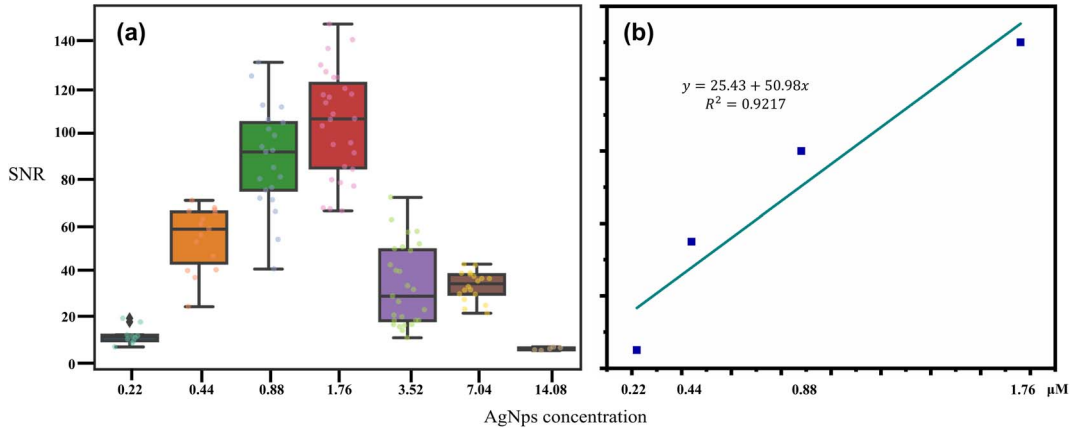

Fig. 4 The variation of the signal-to-noise ratio of SERS spectrum with AgNP concentration, (a) the box diagram of signal-to-noise ratio variation, and (b) the linear correlation diagram of concentration 0.22 to 1.76 μM.

Enhanced validation of AgNPs

AgNPs@normal and AgNPs@KCl were mixed with rhodamine 6G respectively, and the test results are shown in Fig. 3. We can observe that when AgNPs@KCl is combined with KCl, the enhancing impact is about 5 times larger than that when AgNPs@normal is used alone. It is because salt ions can increase AgNP aggregation and improve the enhancing effect.[30] In the following AgNPs and bacteria studies, we employed AgNPs@KCl.

The effect of the AgNP concentration on the enhancement effect

The test results for the mixture of AgNPs@KCl and bacteria at different concentrations are shown in the box diagram in Fig. 4(a). As can be seen, as the concentration of AgNPs@KCl in the region of 0.22–1.76 μM grows, so does the signal-to-noise ratio of the Raman signal. However, there is some activity inhibition of bacteria by AgNPs,[31] so with a concentration of AgNPs above 1.76 μM, the activity of bacteria is affected. This eventually leads to a decrease in the spectral signal-to-noise ratio. It can be seen in Fig. 4(b) that the increase of the signal-to-noise ratio between the concentration 0.22–1.76 μM is linear, with acceptable linearity. We utilized 1.76 μM concentrated AgNPs in the following studies.

Effect of reaction time on the results

AgNPs@KCl and bacteria were mixed and tested according to different reaction times to form a box plot as in Fig. 5(a). The signal-to-noise ratio of Raman spectra grew dramatically in the first 4 h as the binding time between bacteria and AgNPs increased, and stayed at a higher level beyond that period. However, when the reaction time increased, the signal-to-noise ratio of Raman spectra fell after 10 h. There are two reasons for the low spectral signal-to-noise ratio, one is the oxidation of AgNPs by contact with air in the sample and thus loss of enhanced activity,[32] and the other is the inhibitory effect of AgNPs on bacterial activity, which kills and dissolves bacteria

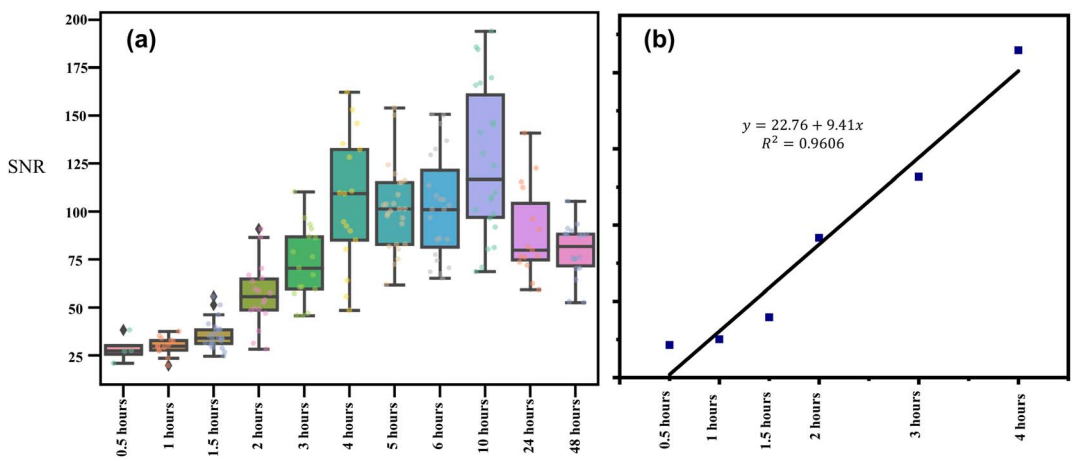

Fig. 5 (a) Box diagram of the relationship between the signal-to-noise ratio and time of AgNPs and bacteria co incubation and (b) correlation curve the between signal-to-noise ratio and incubation time in the first 4 h.

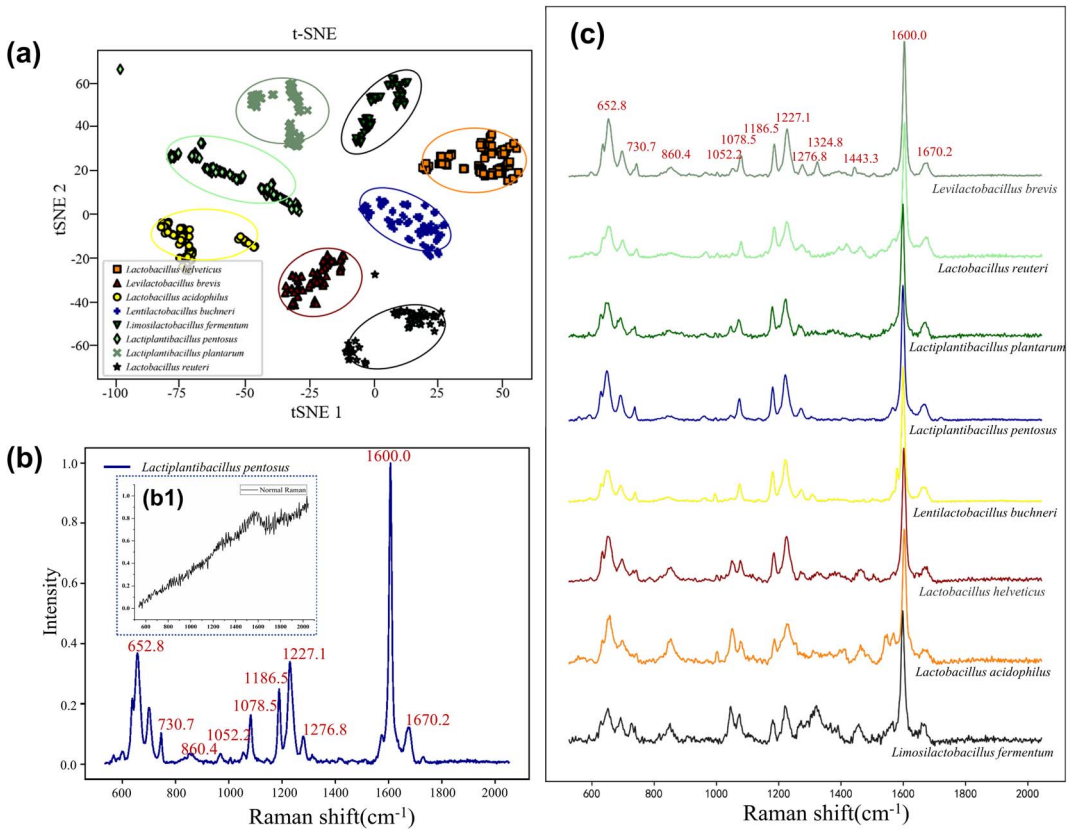

Fig. 6 (a) 2D classification diagram of identification of different bacteria, (b) SERS spectrum of *Lactobacillus pentosus*, (c) list diagram of identification of different bacteria, and (b1) normal bacterial Raman spectrum.

after the prolonged reaction. Therefore, the duration of the later test was set between 4 and 10 h. As shown in the signal-to-noise ratio-time correlation curve of Fig. 5(b), the linearity in the first 4 h is very strong.

Identification of various *Lactobacillus* strains

AgNPs@KCl at a concentration of 1.76 μM and different beer spoilage bacteria were mixed and incubated for 4 h and then tested. In the test, we tested the bacterial MAPPING heat map, and the SERS hotspots were visible when the AgNPs adhered to the bacterial surface (Fig. 1(b)). The following are the results of all bacterial tests: in this study eight beer spoilage bacteria were cultured by brewing. Fig. 6(b1) shows the Raman spectra of *Lactiplantibacillus pentosus* without SERS enhancement, and it can be seen that the spectra have strong fluorescence interference, which makes identification impossible. In contrast, the SERS-enhanced Raman spectra of *Lactiplantibacillus pentosus* in Fig. 6(b) have distinct peaks at 652, 730, 860, 1078, 1227, 1324, 1600, and 1670 cm^{-1}, which greatly enhance the identification rate. Table 1 shows the individual peak positions and their peak attribution. The changes in peak locations of different bacteria between 1000 and 1400 cm^{-1} beams are seen in the enumeration plot (Fig. 6(c)). After downscaling the SERS spectrum data of eight species of beer spoilage bacteria using the t-SNE technique, it can be seen that the distribution of each type of spectra is quite concentrated. The spectral data (in Fig. 6(a)) show clear discrepancies. We used a machine learning technique to build a spectral classification model to examine the enhancing impact of SERS and the degree of difference between the eight categories of spectra. The SVM algorithm was used for the prediction analysis of eight bacteria. The SVM prediction confusion matrix was obtained using a 5-fold cross-validation method[33] (Fig. 7(a)). From the matrix, it can be seen that the identification accuracy of the eight beer spoilage bacteria is high all above 92%. Then the identification accuracy is verified

Table 1 SERS spectral peaks of *Lactobacillus pentosus* and their attribution

Raman shift (cm^{-1})	Peak position attribution
652	δ(COO–)
730	Adenine and polysaccharide
860	C–C telescopic vibration
1078	Carbohydrate δ(CC, CO, and –COH)
1227	Amide III, adenine, and DNA
1324	$\nu(NH_2)$, adenine, and DNA
1600	Amide II, ν(CN), and γ(NH)
1670	Amide I

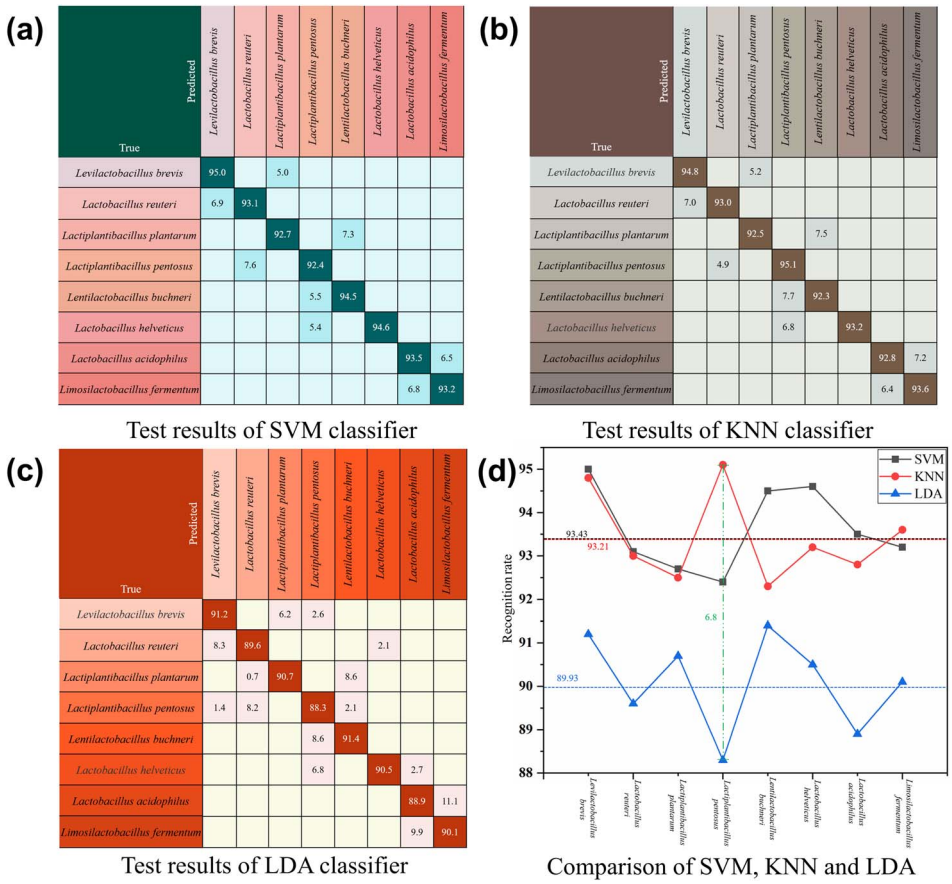

Fig. 7 (a) The SVM confusion matrix results. (b) The KNN confusion matrix results. (c) The LDA confusion matrix results. (d) Comparison of SVM, KNN and LDA.

using KNN and LDA algorithms (KNN and LDA prediction confusion matrix is obtained (Fig. 7(b and c))). From Fig. 7(d), it can be seen that the three machine learning algorithms have similar accuracy rates of about 90%, and all of them can identify eight beer spoilage bacteria well. The SVM algorithm identified a mean value of 93.43% similar to that of the KNN algorithm, 93.21%, and better than that of the LDA algorithm, 89.93%. The results indicate that beer spoilage bacteria can be well identified using all three machine learning algorithms, and the SVM and KNN algorithms have some recognition accuracy advantages over LDA.

Test spectral stability analysis

Spectrum stability is the cornerstone of further data processing. This study employs *Levilactobacillus brevis* as an example to validate spectral stability. The spectra were collected 15 times in a row under test conditions of 1 mW laser power and 2 s integration time. Finally, the spectral enumeration was constructed as shown in Fig. 8(a). The Raman spectral peak positions did not wander over the 15 times of continuous sampling testing, and the overall spectral stability was good. It demonstrates that the experimental results of this work are reliable.

Validation analysis of fermentation-contaminated beer

SERS detection of contaminated beer bacteria in a simulated environment. Three bacteria were selected from the 100× objective field to test the SERS spectra and the spectral features were compared with the database of eight beer spoilage bacteria built by the SVM machine learning algorithm (Fig. 8(b), the SVM algorithm was chosen because it has the best identification results among the three algorithms). It can be seen from Fig. 8(c–e) that the algorithm has a good ability to distinguish the SERS spectra of different bacteria. Among them, Fig. 8(c and d) show a good recognition accuracy (both around 90%). In contrast, Fig. 8(e) shows a poor recognition rate of 61%, because this bacterium is distinguished from the other 8 beer spoilage bacteria and its SERS spectrum information is not included in the database. Moreover, from its bacterial morphology, the bacterium was spherical in shape and was not *Lactobacillus*. The experimental results were validated using plate scribe culture and the subsequent results showed that *Lactiplantibacillus plantarum*, and *Levilactobacillus brevis* two beer spoilage bacteria were indeed present in this sample. The validation results indicated that SERS spectroscopy of the beer spoilage bacteria using an aluminized chip combined with AgNP wrapping, followed by machine learning algorithms allowed for

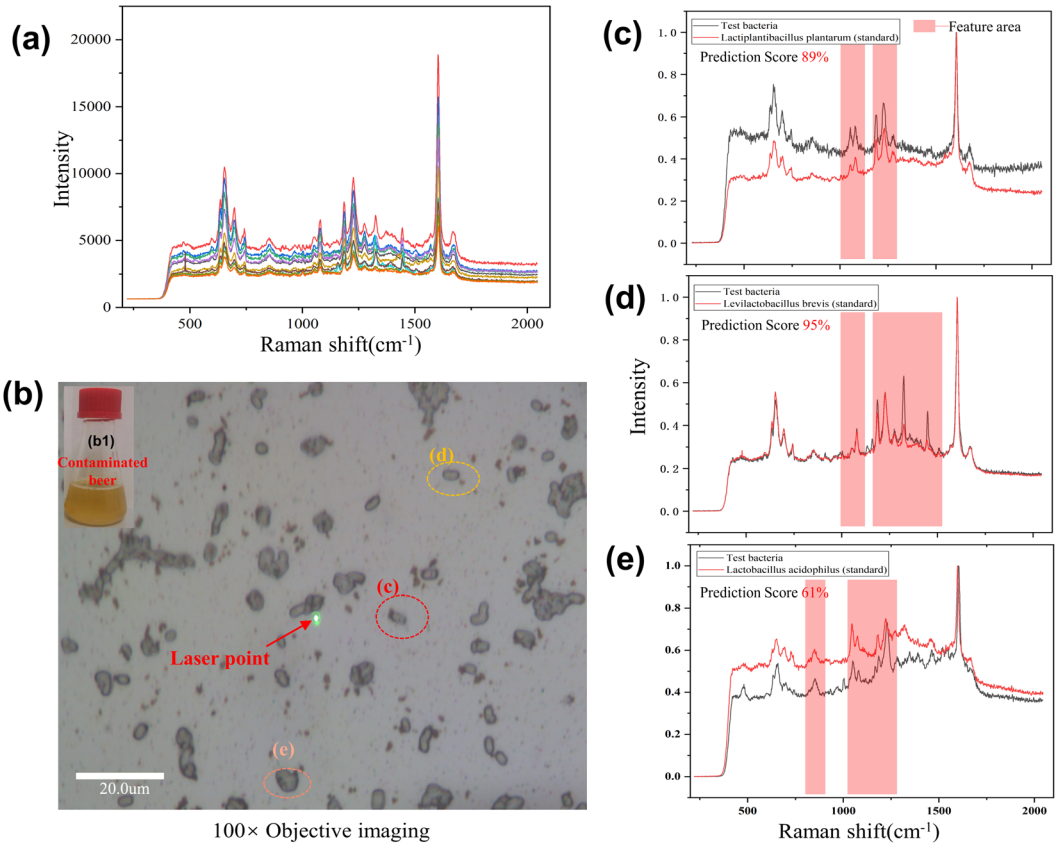

Fig. 8 (a) Spectrum stability test chart. (b) 100× objective imaging of tested bacteria. (b1) Contaminated beer. (c) Comparison of the spectral differences between testing bacteria and *Lactiplantibacillus plantarum*. (d) Comparison of the spectral differences between testing bacteria and *Levilactobacillus brevis*. (e) Comparison of the spectral differences between testing bacteria and *Lactobacillus acidophilus*.

rapid identification and analysis of the bacteria. This has significant implications for the rapid identification of beer spoilage bacteria.

Conclusion

In conclusion, to improve the sensitivity and signal-to-noise ratio of bacterial SERS detection and to accomplish quick identification of spoilage bacteria using the label-free SERS technique as a starting point, we collected eight species of beer spoilage bacteria. The test substrate was an aluminized chip, and the effects of AgNP concentration, AgNPs, and bacterial action time on the results were explored. Finally, by combining the t-SNE reduced dimensional analysis algorithm, SVM, KNN, and LDA machine learning algorithms, the influence of the approach on the final recognition rate was investigated further. When KCl is introduced to the AgNP manufacturing process, the AgNP concentration is 1.76 μM, and the reaction time with bacteria is 4 h; the experimental findings show that a high signal-to-noise ratio spectrum may be obtained. Furthermore, with an accuracy of roughly 90%, all three machine learning algorithms performed well in identifying beer spoilage bacteria. With a mean value of 93.43%, SVM has the highest accuracy of the group. Finally, two beer spoilage bacteria were chosen and added to uncontaminated beer for a mixed culture to confirm the method's viability. A comparison of the SERS spectrum's similarity to those in the database was performed in the end, and the results demonstrated that SERS spectra of known spoilage bacteria could be accurately identified. The stability and repeatability of the spectra are good. The downside is that germs outside the database cannot be accurately detected, necessitating constant database expansion.

Overall, the current work has enormous potential for advancement. An aluminized chip was employed to further boost the signal strength after the specifics of the investigation into the examination of many components of SERS-enhanced bacteria were examined. The accuracy of machine learning detection of beer spoilage bacteria was further enhanced by the strong suppression of fluorescence interference of the bacteria and the acquisition of SERS spectra of bacteria with significantly higher signal-to-noise ratios than that in other studies. The technology can indeed identify the target spoilage bacteria from simulated samples, according to the final validation studies. This is useful for the rapid detection of beer spoilage bacteria during the brewing process.

Author contributions

Lindong Shang: conceptualization, methodology, data curation, writing – original draft. Lei Xu: methodology, writing – original

draft. Yu Wang: conceptualization, writing – original draft. Kunxiang Liu: conceptualization, writing – review & editing. Peng Liang: formal analysis, writing – review & editing. Shuangjun Zhou: data curation, writing – review & editing. Fuyuan Chen: conceptualization, writing – review & editing. Hao Peng: conceptualization, writing – review & editing. Chunyang Zhou: conceptualization, writing – review & editing. Zhenming Lu: conceptualization, supervision. Bei Li: visualization, supervision.

Conflicts of interest

The authors declare that they have no known competing financial interests or personal relationships that could have appeared to influence the work reported in this paper.

Acknowledgements

National Key R & D Program "International Cooperation in Science and Technology Innovation between Governments/ Cooperation in Science and Technology Innovation between Hong Kong, Macao and Tai-wan" (SQ2018YFE010810).

References

1 K. Suzuki, K. Iijima, K. Sakamoto, M. Sami and H. Yamashita, *J. Inst. Brew.*, 2006, **112**, 173–191.
2 K. Sakamoto and W. N. Konings, *Int. J. Food Microbiol.*, 2003, **89**, 105–124.
3 Y. Deng, J. Liu, H. Li, L. Li, J. Tu, H. Fang, J. Chen and F. Qian, *J. Inst. Brew.*, 2014, **120**, 127–132.
4 C. Garofalo, A. Osimani, V. Milanović, M. Taccari, L. Aquilanti and F. Clementi, *J. Food Sci.*, 2015, **80**, M2845–M2852.
5 H. Peng and I. A. Chen, *ACS Nano*, 2019, **13**, 1244–1252.
6 Z.-H. Cheng, X. Liu, S.-Q. Zhang, T. Yang, M.-L. Chen and J.-H. Wang, *Anal. Chem.*, 2019, **91**, 12094–12099.
7 R. Zgheib, H. Anani, M. M. Meng, M. Mailhe, D. Ricaboni, A. Morand, A. Caputo, S. I. Traore, A. Fontanini and N. Armstrong, *Int. J. Syst. Evol. Microbiol.*, 2021, **71**, 004819.
8 L. X. Coggins, I. Larma, A. Hinchliffe, R. Props and A. Ghadouani, *Water Res.*, 2020, **169**, 115243.
9 P. Shah and Z.-W. Wang, *Sci. Total Environ.*, 2019, **689**, 269–277.
10 L.-P. Sun, Y. Huang, T. Huang, Z. Yuan, W. Lin, Z. Sun, M. Yang, P. Xiao, J. Ma, W. Wang, Y. Zhang, Z. Liu and B.-O. Guan, *Anal. Chem.*, 2019, **91**, 14141–14148.
11 M. Petersen, Z. Yu and X. Lu, *Biosensors*, 2021, **11**(6), 187.
12 M. Schmitt and J. Popp, *J. Raman Spectrosc.*, 2006, **37**, 20–28.
13 H.-b. Liu, X.-j. Du, Y.-X. Zang, P. Li and S. Wang, *J. Agric. Food Chem.*, 2017, **65**, 10290–10299.
14 Y. Pang, N. Wan, L. Shi, C. Wang, Z. Sun, R. Xiao and S. Wang, *Anal. Chim. Acta*, 2019, **1077**, 288–296.
15 D. Vaitiekūnaitė and V. Snitka, *Microorganisms*, 2021, **9**, 1969.
16 L. Li, R. Hou, W. Shen, Y. Chen, S. Wu, Y. Wang, X. Wang, Z. Yuan and D. Peng, *Food Chem.*, 2021, **363**, 129465.
17 R. M. Renuka, J. Achuth, H. R. Chandan, M. Venkataramana and K. Kadirvelu, *New J. Chem.*, 2018, **42**, 10807–10817.
18 E. Akanny, A. Bonhommé, C. Commun, A. Doleans-Jordheim, C. Farre, F. Bessueille, S. Bourgeois and C. Bordes, *J. Raman Spectrosc.*, 2020, **51**, 619–629.
19 S. Efrima and B. V. Bronk, *J. Phys. Chem. B*, 1998, **102**, 5947–5950.
20 P. Wang, S. Pang, J. Chen, L. McLandsborough, S. R. Nugen, M. Fan and L. He, *Analyst*, 2016, **141**, 1356–1362.
21 P. Chuesiang, V. Ryu, U. Siripatrawan, L. McLandsborough and L. He, *LWT–Food Sci. Technol.*, 2021, **150**, 111962.
22 M. Kashif, M. I. Majeed, H. Nawaz, N. Rashid, M. Abubakar, S. Ahmad, S. Ali, H. Hyat, S. Bashir, F. Batool, S. Akbar and M. A. Anwar, *Spectrochim. Acta, Part A*, 2021, **261**, 119989.
23 L.-J. Chai, M.-N. Shen, J. Sun, Y.-J. Deng, Z.-M. Lu, X.-J. Zhang, J.-S. Shi and Z.-H. Xu, *Food Microbiol.*, 2020, **92**, 1035V59.
24 N. Leopold and B. Lendl, *J. Phys. Chem. B*, 2003, **107**, 5723–5727.
25 L. Sepunaru, K. Tschulik, C. Batchelor-McAuley, R. Gavish and R. G. Compton, *Biomater. Sci.*, 2015, **3**, 816–820.
26 F. Anowar, S. Sadaoui and B. Selim, *Comput. Sci. Rev.*, 2021, **40**, 100378.
27 V. K. Chauhan, K. Dahiya and A. Sharma, *Artif. Intell. Rev.*, 2019, **52**, 803–855.
28 G. Guo, H. Wang, D. Bell, Y. Bi and K. Greer, KNN model-based approach in classification, *OTM Confederated International Conferences "On the Move to Meaningful Internet Systems"*, Springer, Berlin, Heidelberg, 2003, pp. 986–996.
29 L.-F. Chen, H.-Y. M. Liao, M.-T. Ko, J.-C. Lin and G.-J. Yu, *Pattern Recognit.*, 2000, **33**, 1713–1726.
30 K. Li, A. Liang, C. Jiang, F. Li, Q. Liu and Z. Jiang, *Talanta*, 2012, **99**, 890–896.
31 M. Rai, A. Yadav and A. Gade, *Biotechnol. Adv.*, 2009, **27**, 76–83.
32 H. M. M. Ibrahim, *World J. Microbiol. Biotechnol.*, 2015, **31**, 1049–1060.
33 T. Fushiki, *Stat Comput.*, 2011, **21**, 137–146.

